

Scalarized charged black holes in the Einstein-Maxwell-Scalar theory with two U(1) fields

Yun Soo Myung^{a*} and De-Cheng Zou^{a,b†}

^aInstitute of Basic Sciences and Department of Computer Simulation, Inje University
Gimhae 50834, Korea

^bCenter for Gravitation and Cosmology and College of Physical Science and Technology,
Yangzhou University, Yangzhou 225009, China

Abstract

We investigate scalarized charged black holes in the Einstein-Maxwell-Scalar theory with two U(1) fields inspired by the $N = 4$ supergravity. From the onset of the spontaneous scalarization (tachyonic instability of Reissner-Nordström black hole), these black holes are classified by the number of $n = 0, 1, 2, \dots$, where $n = 0$ is called the fundamental black hole and $n = 1, 2, \dots$ denote the n -excited black holes. Adopting radial perturbations, we show that the $n = 0$ black hole is stable against the $s(l = 0)$ -mode scalar perturbation, whereas the $n = 1, 2$ excited black holes are unstable. This implies that the $n = 0$ black hole is considered as an endpoint of the Reissner-Nordström black hole.

*e-mail address: ysmyoung@inje.ac.kr

†e-mail address: dczou@yzu.edu.cn

1 Introduction

Recently, the inclusion of non-minimal scalar couplings with coupling parameter α has induced the instability of Schwarzschild black holes and thus, led to scalarized black holes [1, 2, 3]. This is known to be a phenomena of spontaneous scalarization, a way of providing black holes with scalar hair. Also, non-minimal coupling to the Maxwell invariant [Einstein-Maxwell-scalar(EMS) theory] has accommodated a phenomena of spontaneous scalarization of Reissner-Nodström (RN) black holes [4]. It is worth noting that the existence line separating RN black holes from scalarized charged black holes is universal in the sense that the various scalar couplings $\{f(\phi)\}$ to the Maxwell invariant are identical in the linearized approximation [5].

On the other hand, an analysis of dilatonic versus scalarized couplings has shown that two have provided charged black holes with scalar hair with analytical and numerical forms, but the former does not accommodate RN black holes, whereas the latter has a smooth extremal scalarized black hole by considering dyonic RN black holes [6]. This implies a comparative difference between dilatonic and scalarized couplings in the EMS theory.

In this work, we wish to introduce the EMS theory with different scalar couplings to two U(1) field strengths for realizing another spontaneous scalarization because the same coupling makes no difference. This theory is inspired by the bosonic sector of $N = 4$ supergravity which has admitted an analytically dilatonic black hole with a fixed scalar including an extremal black hole. There were many testing of stringy black holes with fixed scalars, being different from minimally coupled (free) scalars. Such testings have included computation of the greybody factor for a propagating scalar around an extremal black holes: $\sigma_s^{\text{free}} \rightarrow 4\pi$ and $\sigma_s^{\text{fixed}} \rightarrow 4\pi\omega^2 \rightarrow 0$ in the low-energy limit ($\omega \rightarrow 0$), implying that a suppression of Hawking radiation occurred in the fixed scalar, compared to the free scalar [7, 8, 9]. For a fixed scalar, a scalar $\phi_{\text{fixed}}^\infty$ at infinity is independent of the value of scalar $\phi(r_+) = \phi_{\text{fixed}}^0(q)$ on the horizon [10, 11]. It is proposed that a fixed scalar in the dilatonic black holes is similar to the scalar hair in the $n = 0, 1, 2$ scalarized black holes.

Therefore, it is quite interesting to compare the fixed scalar in dilatonic black holes with the scalar hair in the sclarized black holes. Introducing radial perturbations, we wish to show that the $n = 0$ black hole is stable against the $s(l = 0)$ -mode scalar perturbation, while the $n = 1, 2$ excited black holes are unstable.

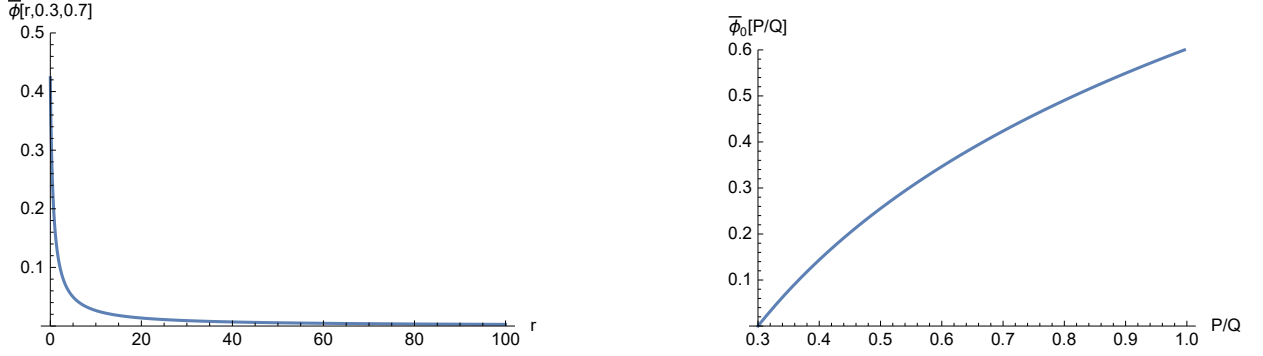


Figure 1: (Left) The dilaton $\bar{\phi}(r, Q = 0.3, P = 0.7)$ as functions of $r \in [r_+ = 0, 100]$. The dilaton takes a value of $\bar{\phi} = 0.42365$ on the horizon at $r = 0$ and it vanishes asymptotically. (Right) The dilaton $\bar{\phi}_0(P/Q)$ on the horizon at $r = r_+ = 0$ with $Q = 0.3$, showing a fixed scalar.

2 Instability of RN black hole

First of all, we introduce the bosonic action for $N = 4$ supergravity [7, 8, 9]

$$S_{N4} = \frac{1}{16\pi} \int d^4x \sqrt{-g} \left[R - 2\partial_\mu \phi \partial^\mu \phi - e^{-2\phi} F^2 - e^{2\phi} H^2 \right], \quad (1)$$

where ϕ plays the role of dilaton and $F = dA$ and $H = dB$ are two U(1) field strengths. The RN-type black hole without scalar hair could not found from (1). An analytic black hole solution is given by

$$ds_{N4BH}^2 = -\frac{1}{H_1 H_2} dt^2 + H_1 H_2 \left(dr^2 + r^2 d\Omega_2^2 \right) \quad (2)$$

and

$$e^{2\bar{\phi}} = \frac{H_2}{H_1}, \quad \bar{F} = \frac{1}{\sqrt{2}} dH_1^{-1} \wedge dt, \quad \bar{H} = \frac{1}{\sqrt{2}} dH_2^{-1} \wedge dt \quad (3)$$

with two harmonic functions

$$H_1 = 1 + \frac{\sqrt{2}Q}{r}, \quad H_2 = 1 + \frac{\sqrt{2}P}{r}. \quad (4)$$

The event horizon is located at $r_+ = 0$ and a fixed scalar $\bar{\phi}$ is defined as the special massless field whose value on the horizon is fixed by the U(1) charges Q and P , leading to $\lim_{r \rightarrow 0} \bar{\phi} = 0.5 \ln \left[\frac{P}{Q} \right]$. In case of $P = Q$ (extremal black hole), one finds that $\bar{\phi} = 0$. Fig. 1 shows that the dilaton is a fixed scalar, being similar to scalar hair. Considering the radial

perturbations around (2), the linearized equation for s -mode dilaton $\delta\phi(t, r) = \tilde{\varphi}(r)e^{-i\omega t}$ is given by

$$\left[\frac{1}{r^2} \frac{d}{dr} \left(r^2 \frac{d}{dr} \right) + \omega^2 (H_1 H_2)^2 - \frac{4(P+Q)^2}{r^2 (\sqrt{2P} + \sqrt{2Q} + 2r)^2} \right] \tilde{\varphi}(r) = 0, \quad (5)$$

which turned out to be stable because of $\omega > 0$.

Now let us obtain the action for the Einstein-Maxwell-Scalar theory with two U(1) fields (EMSN4 theory) induced by $N = 4$ supergravity by replacing 2ϕ in the exponents with $\alpha\phi^2$ on (1)

$$S_{\text{EMSN4}} = \frac{1}{16\pi} \int d^4x \sqrt{-g} \left[R - 2\partial_\mu \phi \partial^\mu \phi - e^{-\alpha\phi^2} F^2 - e^{\alpha\phi^2} H^2 \right], \quad (6)$$

where α is a scalar coupling parameter.

We derive the Einstein equation from the action (6)

$$G_{\mu\nu} = 2\partial_\mu \phi \partial_\nu \phi - (\partial\phi)^2 g_{\mu\nu} + 2T_{\mu\nu}^{U(1)} \quad (7)$$

with $G_{\mu\nu} = R_{\mu\nu} - (R/2)g_{\mu\nu}$ and

$$T_{\mu\nu}^{U(1)} = e^{-\alpha\phi^2} \left(F_{\mu\rho} F_{\nu}{}^\rho - \frac{F^2}{4} g_{\mu\nu} \right) + e^{\alpha\phi^2} \left(H_{\mu\rho} H_{\nu}{}^\rho - \frac{H^2}{4} g_{\mu\nu} \right). \quad (8)$$

Two Maxwell equations take the forms

$$\nabla^\mu F_{\mu\nu} - 2\alpha\phi \nabla^\mu(\phi) F_{\mu\nu} = 0, \quad (9)$$

$$\nabla^\mu H_{\mu\nu} + 2\alpha\phi \nabla^\mu(\phi) H_{\mu\nu} = 0. \quad (10)$$

The scalar equation is given by

$$\square\phi + \frac{\alpha}{2} \left(F^2 e^{-\alpha\phi^2} - H^2 e^{\alpha\phi^2} \right) \phi = 0. \quad (11)$$

First of all, we would like to mention the RN-type black hole solution without scalar hair

$$ds_{\text{RN-type}}^2 = \bar{g}_{\mu\nu} dx^\mu dx^\nu = -f(r) dt^2 + \frac{dr^2}{f(r)} + r^2 d\Omega_2^2, \quad f(r) = 1 - \frac{2M}{r} + \frac{Q^2 + P^2}{r^2} \quad (12)$$

which is obtained, irrespective of any value of α . Here, we have that $\bar{\phi} = 0$, $\bar{A}_t = Q/r$, and $\bar{B}_t = P/r$. Two horizons are determined as $r_\pm = M[1 \pm \sqrt{1 - (q^2 + p^2)}]$ with $q = Q/M$ and $p = P/M$ by imposing $f(r) = 0$. For $M = 1$, one has $P = p$ and $Q = q$. Hereafter, we consider only the region on and outside the outer horizon ($r \geq r_+$). Further, we would like to mention that the dyonic RN black hole takes the same form as (12) [6].

Let us consider the perturbations around the background values

$$g_{\mu\nu} = \bar{g}_{\mu\nu} + h_{\mu\nu}, \quad \phi = 0 + \delta\phi, \quad F_{\mu\nu} = \bar{F}_{\mu\nu} + f_{\mu\nu}, \quad H_{\mu\nu} = \bar{H}_{\mu\nu} + \tilde{f}_{\mu\nu}, \quad (13)$$

where

$$f_{\mu\nu} = \partial_\mu a_\nu - \partial_\nu a_\mu, \quad \tilde{f}_{\mu\nu} = \partial_\mu b_\nu - \partial_\nu b_\mu. \quad (14)$$

Now, we derive their linearized equations as

$$\delta G_{\mu\nu}(h) = 2\delta T_{\mu\nu}^{U(1)}, \quad (15)$$

$$\bar{\nabla}^\mu f_{\mu\nu} = 0, \quad \bar{\nabla}^\mu \tilde{f}_{\mu\nu} = 0, \quad (16)$$

$$\left[\bar{\square} + \frac{\alpha(P^2 - Q^2)}{r^4} \right] \delta\phi = 0, \quad (17)$$

where

$$\delta G_{\mu\nu} = \delta R_{\mu\nu} - \frac{1}{2}\bar{g}_{\mu\nu}\delta R - \frac{1}{2}\bar{R}h_{\mu\nu}, \quad (18)$$

$$\begin{aligned} \delta T_{\mu\nu}^{U(1)} &= \bar{F}_\nu{}^\rho f_{\mu\rho} + \bar{F}_\mu{}^\rho f_{\nu\rho} - \bar{F}_{\mu\rho}\bar{F}_{\nu\sigma}h^{\rho\sigma} + \frac{1}{2}(\bar{F}_{\kappa\eta}f^{\kappa\eta} - \bar{F}_{\kappa\eta}\bar{F}^{\kappa}{}_\sigma h^{\eta\sigma})\bar{g}_{\mu\nu} - \frac{1}{4}\bar{F}^2 h_{\mu\nu} \\ &+ \bar{H}_\nu{}^\rho \tilde{f}_{\mu\rho} + \bar{H}_\mu{}^\rho \tilde{f}_{\nu\rho} - \bar{H}_{\mu\rho}\bar{H}_{\nu\sigma}h^{\rho\sigma} + \frac{1}{2}(\bar{H}_{\kappa\eta}\tilde{f}^{\kappa\eta} - \bar{H}_{\kappa\eta}\bar{H}^{\kappa}{}_\sigma h^{\eta\sigma})\bar{g}_{\mu\nu} \\ &- \frac{1}{4}\bar{H}^2 h_{\mu\nu}. \end{aligned} \quad (19)$$

In analyzing the stability of the RN-type black hole in the EMS theory with two U(1) fields, we first consider the linearized equations (15) and (16) because three perturbations of metric $h_{\mu\nu}$ and vectors a_μ and b_μ are coupled. These are similar to the linearized equations for the Einstein-Maxwell theory with single U(1) field H [12]. For the odd-parity perturbations, one found the Zerilli-Moncrief equation which describes two physical DOF (degrees of freedom) propagating around the RN black hole [13, 14]. Also, the even-parity perturbations with two physical DOF were studied in [15, 16]. It turns out that the RN black hole is stable against these perturbations.

In our case, a massless spin-2 mode starts with $l = 2$, while two massless spin-1 mode begin with $l = 1$. The EMS theory with two U(1) provides 7(=2+2+2+1) DOF propagating around the RN-type background. We hope that the RN-type black hole is still stable against full tensor-vector perturbations.

Now, we focus on the the linearized scalar equation (17) which determines totally the instability of RN-type black hole found from the EMS theory with two U(1) fields. From

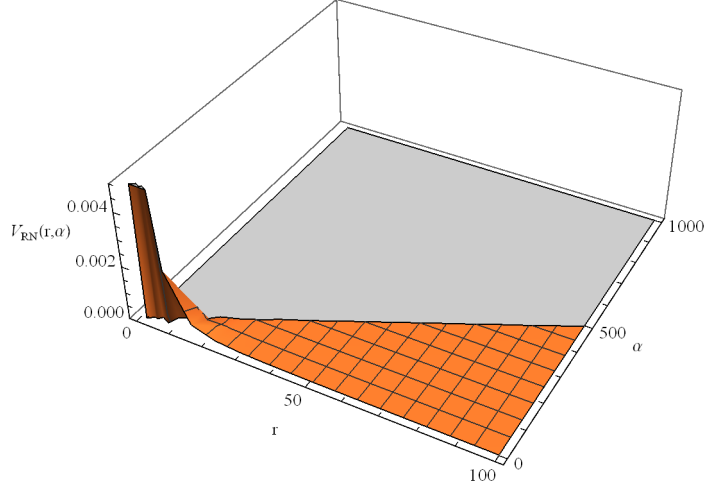


Figure 2: The 3D potential $V_{\text{RN}}(r, \alpha)$ as functions of $r \in [r_+ = 1.648, 100]$ and $\alpha \in [0, 1000]$ with $p = 0.7$, $q = 0.3$, and $l = 0$. The shaded region denotes negative region between $r = r_+$ and $r = r_{\text{out}} = (p^2 + q^2) + \alpha(p^2 - q^2)/2$.

now on, we call RN-type as RN for simplicity. Introducing

$$\delta\varphi(t, r, \theta, \phi) = \int \sum_{lm} \varphi(r) Y_{lm}(\theta) e^{im\phi} e^{-i\omega t} d\omega, \quad \varphi(r) = \frac{u(r)}{r} \quad (20)$$

equation (17) takes the Schrödinger-equation with the tortoise coordinate r_*

$$\frac{d^2 u(r)}{dr_*^2} + [\omega^2 - V_{\text{RN}}(r)] u(r) = 0, \quad r_* = \int \frac{dr}{f(r)}. \quad (21)$$

Here, the potential is given by

$$V_{\text{RN}}(r) = f(r) \left[\frac{2M}{r^3} + \frac{l(l+1)}{r^2} - \frac{2(Q^2 + P^2)}{r^4} - \frac{\alpha(P^2 - Q^2)}{r^4} \right], \quad (22)$$

where the case of $P^2 > Q^2$ induces the tachyonic instability depending on the coupling parameter α . Also, the case of $P^2 = Q^2$ implies no coupling effectively. We wish to delete the other case of $P^2 < Q^2$ because it induces a positive definite potential, leading to the stable RN black hole. In addition, the case of the same coupling leads to the last term of $-\alpha(P^2 + Q^2)/r^4$, which makes no difference when comparing with the EMS theory. This is the reason why we consider the different scalar couplings as $e^{-\alpha\phi^2} F^2$ and $e^{\alpha\phi^2} H^2$. In Fig. 2, we display the (r, α) -dependent potentials for given $l = 0$, $M = 1$ and $p = 0.7, q = 0.3$ (a non-extremal RN black hole). The negative (shaded) region appears between $r = r_+$

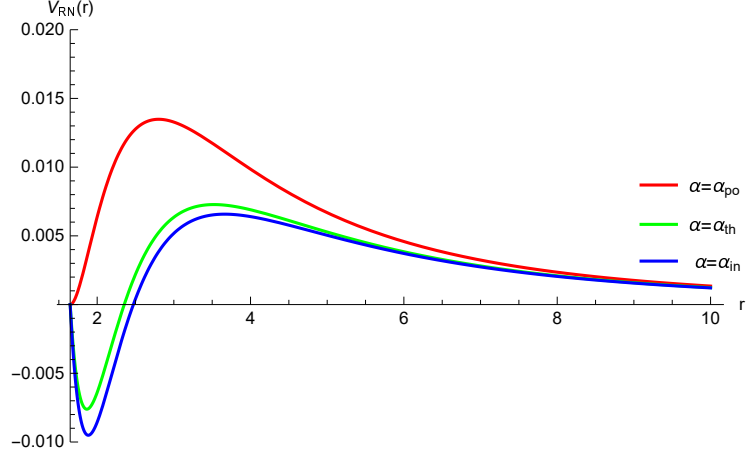


Figure 3: The α -dependent potentials as function of $r \in [r_+, 10]$ with the outer horizon radius $r_+ = 1.648(p = 0.7, q = 0.3)$ and $l = 0$. From the top, each curve represents the potential $V_{\text{RN}}(r)$ of a scalar field for $\alpha_{\text{po}} = 5.3404$ (sufficient condition for stability), $\alpha_{\text{th}} = 8.8646$ (threshold of instability), $\alpha_{\text{in}} = 9.4606$ (sufficient condition for instability), respectively.

and $r = r_{\text{out}} = (p^2 + q^2) + \alpha(p^2 - q^2)/2$, whose region can be used for computing the discrete resonant spectrum ($\{\alpha_n\}$) when employing the WKB method. The $s(l = 0)$ -mode is allowed for the scalar perturbation and it is regarded as an important mode to test the stability of the RN black hole. Hereafter, we consider this mode only.

The sufficient condition of $\int_{r_+}^{\infty} dr [V_{\text{RN}}(r)/f(r)] < 0$ for instability [17] leads to the bound as

$$\alpha > \alpha_{\text{in}}(p, q) = \frac{-2(p^2 + q^2) + 3(1 + \sqrt{1 - p^2 - q^2})}{p^2 - q^2}, \quad (23)$$

where we note that $V_{\text{RN}}(r)/f(r)$ differs from $V_{\text{RN}}(r)$ in Fig. 3. On the other hand, by observing the potential (22), the positive definite potential without negative region could be found when imposing the bound

$$\alpha \leq \alpha_{\text{po}}(p, q) = \frac{-2(p^2 + q^2) + 2(1 + \sqrt{1 - p^2 - q^2})}{p^2 - q^2}, \quad (24)$$

which is called the sufficient condition for stability. Fig. 3 suggests that the threshold of instability α_{th} is between $\alpha_{\text{po}} = 5.3404$ and $\alpha_{\text{in}} = 9.4606$ for $p = 0.7$ and $q = 0.3$. To determine the threshold of instability α_{th} , one has to solve the second-order differential

equation numerically

$$\frac{d^2 u}{dr_*^2} - \left[\Omega^2 + V_{\text{RN}}(r) \right] u(r) = 0, \quad (25)$$

which allows an exponentially growing mode of $e^{\Omega t}$ ($\omega = i\Omega$) as an unstable mode. Here we choose two boundary conditions: a normalizable solution of $u(\infty) \sim e^{-\Omega r_*}$ at infinity and a solution of $u(r_+) \sim (r - r_+)^{\Omega r_+}$ near the outer horizon. We find that the threshold ($\Omega = 0$) of instability is located at $\alpha_{\text{th}} = 8.86464$ for $p = 0.7$ and $q = 0.3$. This implies that for given $p = 0.7$ and $q = 0.3$, the RN black hole is unstable for $\alpha > \alpha_{\text{th}}$ (See Fig. 10), while it is stable for $\alpha < \alpha_{\text{th}}$. The other way of obtaining α_{th} is to solve the static linearized equation directly because $\alpha_{\text{th}} = \alpha_{n=0}^{\text{E}}$.

We consider the static scalar perturbed equation on the RN black hole background to identify the $n = 0, 1, 2$ black holes as

$$\frac{1}{r^2} \frac{d}{dr} \left[r^2 f(r) \frac{d\varphi(r)}{dr} \right] - \left[\frac{l(l+1)}{r^2} - \frac{\alpha(P^2 - Q^2)}{r^4} \right] \varphi(r) = 0 \quad (26)$$

which describes an eigenvalue problem: for a given $l = 0$, requiring an asymptotically vanishing, smooth scalar field selects a discrete set of $n = 0, 1, 2, \dots$. Actually, these determine the bifurcation points (discrete resonant spectrum: $\{\alpha_n^{\text{E}}\}$) numerically. For this purpose, one may transform (26) to the Legendre equation whose exact solution is given by

$$\varphi(r) = P_u \left[1 + \frac{2(P^2 + Q^2)(r - r_+)}{r(r_+^2 - Q^2 - P^2)} \right], \quad u = \frac{1}{2} \left[\sqrt{1 - 4\alpha \left(\frac{P^2 - Q^2}{P^2 + Q^2} \right)} - 1 \right] \quad (27)$$

with the Legendre function P_u . Here, we point out that there was a wrong transformation to the Legendre equation in [6]. For four parameters of α , $P(> Q)$, Q , r_+ , the function $\varphi(r)$ approaches a constant non-zero values asymptotically: $\varphi(r) \rightarrow \varphi_\infty = {}_2F_1[\dots] + \mathcal{O}(1/r)$ with ${}_2F_1[\dots]$ the hypergeometric function. Finding $\{\alpha_n^{\text{E}}\}$ is equivalent to obtaining the zeros of ${}_2F_1[\dots]$. So, one has to solve the following equation to find bifurcation points ($\{\alpha_n^{\text{E}}\}$):

$${}_2F_1 \left[1 - u, u + 1, 1, \frac{p^2 + q^2}{2(p^2 + q^2 - 1 - \sqrt{1 - p^2 - q^2})} \right] \Big|_{\{p=0.7, q=0.3\}} = 0. \quad (28)$$

We obtain $\{\alpha_n^{\text{E}}\}$ numerically and list it in Table 1. We confirm a relation of $\alpha_{\text{th}} = \alpha_0^{\text{E}}$. We plot $\varphi(r)$ as a function of r with three $\alpha = \alpha_0^{\text{E}}$, α_1^{E} , α_2^{E} whose forms can be found from Fig. 4. These solutions are classified by the order number $n = 0, 1, 2$ which is identified

n	0	1	2	3	4	5	6	7	8	9	10
α_n^E	8.86464	44.6633	109.071	202.111	323.754	474.031	652.932	860.457	1096.61	1361.38	1654.78
$\alpha_n[(34)]$	8.05054	43.8307	108.235	201.264	322.916	473.193	652.094	859.619	1095.77	1360.54	1653.94

Table 1: Results for α_n^E and α_n for $n = 0, 1, 2, \dots, 10$ branches of scalarized charged black holes with $p = 0.7$ and $q = 0.3$. We confirm that the threshold of instability α_{th} is given by α_0^E .

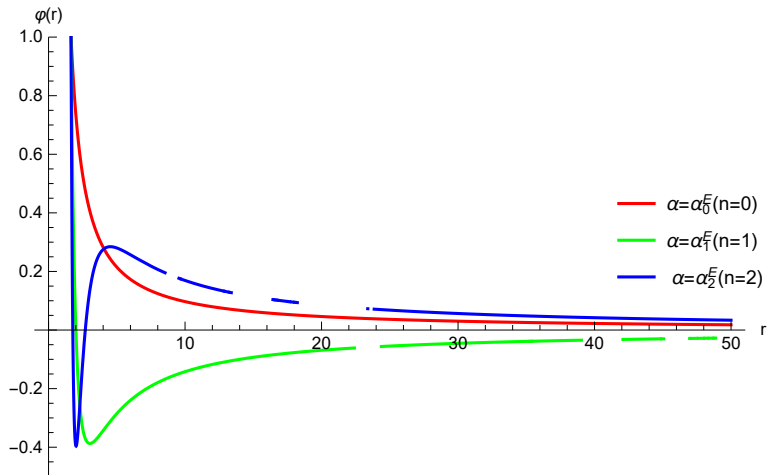


Figure 4: Radial profiles of $\varphi(r)$ as function of $r \in [r_+ = 1.648, 50]$ for the first three perturbed scalar solutions with $p = 0.7$ and $q = 0.3$. These solutions are classified by the order number $n = 0, 1, 2$ which is identified by the number of nodes (zero crossings) for $\varphi(r)$.

by the number of nodes for $\varphi(r)$. It is worth noting that the $n = 0$ scalar cloud without zero crossing will develop the fundamental branch of scalarized charged black hole with $\alpha \geq \alpha_0^E$, while the $n = 1, 2$ scalar clouds with zero crossings will develop the $n = 1, 2$ excited branches of scalarized charged black holes with $\alpha \geq \alpha_1^E, \alpha_2^E$, respectively.

Also, we represent several curves of ${}_2F_1[\dots] = 0$ existing in (α, p) -space (see Fig. 5) whose crossing points with $p = 0.7$ determine $\{\alpha_n^E\}$ in Table 1. For fixed $q = 0.3$ and $\alpha \in [0, 2000]$, the number of crossing points increase as p increases. For example, we have $\alpha_0^E(= \alpha_{\text{th}}) = 838.162$ only for $p = 0.31$, while it includes 23 cases of $\alpha_0^E(= \alpha_{\text{th}}) = 2.59013, \dots, \alpha_{22}^E = 1931.45$ for $p = 0.9$. Importantly, the first curve ($n = 0$) in the left represents an existence one, which means the boundary between RN black hole and scalarized charged black holes. In other words, this curve determines all thresholds of

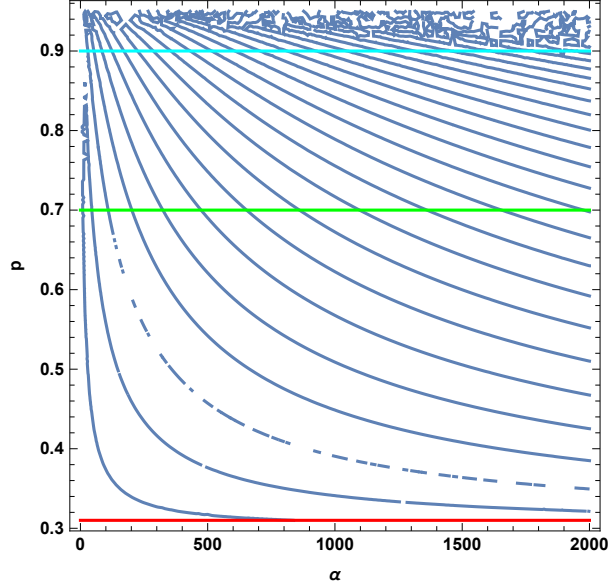


Figure 5: The several curves of ${}_2F_1[\dots] = 0$ as functions of $p \in [0.31, 0.95]$ and $\alpha \in [0, 2000]$ with $q = 0.3$. The curves denote $n = 0, 1, 2, \dots$ from the left to the right. The first curve ($n = 0$) represents the boundary (existence curve) between RN black hole and scalarized charged black holes. A green line implies $p = 0.7$ whose (eleven) crossing points determine α_n^E in Table 1. A. The red and cyan lines denote $p = 0.31$ and $p = 0.9$, respectively.

instability $[\alpha_{\text{th}}(p, q = 0.3)]$ for RN black holes for any $p > 0.3$.

On the other hand, it was proposed that the spatially regular scalar configurations (scalar clouds) described by (25) with $\Omega = 0$ could be investigated analytically by making use of the standard WKB techniques [18]. A standard second-order WKB analysis could be applied for obtaining the bound states of the potential V_{RN} approximately to yield the quantization condition

$$\int_{r_*^{\text{in}}}^{r_*^{\text{out}}} dr_* \sqrt{-V_{\text{RN}}(r_*)} = \left(n - \frac{1}{4}\right)\pi, \quad n = 1, 2, 3, \dots, \quad (29)$$

where r_*^{out} and r_*^{in} are the radial turning points satisfying $V_{\text{RN}}(r_*^{\text{out}}) = V_{\text{RN}}(r_*^{\text{in}}) = 0$. We could express Eq.(29) in terms of the radial coordinate r as

$$\int_{r_{\text{in}}}^{r_{\text{out}}} dr \frac{\sqrt{-V_{\text{RN}}(r)}}{f(r)} = \left(n - \frac{1}{4}\right)\pi, \quad n = 1, 2, 3, \dots, \quad (30)$$

where radial turning points $\{r_{out}, r_{in}\}$ are determined by the two conditions (see Fig. 2)

$$1 - \frac{2M}{r_{in}} + \frac{P^2 + Q^2}{r_{in}^2} = 0, \quad \frac{2M}{r_{out}^3} - \frac{2(P^2 + Q^2)}{r_{out}^4} - \frac{\alpha(P^2 - Q^2)}{r_{out}^4} = 0, \quad (31)$$

which admit

$$r_{in} = r_+, \quad r_{out} = p^2 + q^2 + \frac{\alpha(p^2 - q^2)}{2}. \quad (32)$$

For large α ($r_{out} \rightarrow \infty$), the WKB integral (30) could be approximated by neglecting the first three terms in (22) as

$$\sqrt{\alpha} \int_{r_+}^{\infty} dr \sqrt{\frac{P^2 - Q^2}{r^4 f(r)}} = \left(n + \frac{3}{4}\right)\pi, \quad n = 0, 1, 2, \dots, \quad (33)$$

which could be integrated analytically to yield

$$\alpha_n(p, q) = \left(\frac{p^2 + q^2}{p^2 - q^2}\right) \left[\frac{\pi \left(n + \frac{3}{4}\right)}{\ln \left[\frac{\sqrt{1-p^2-q^2}}{1-\sqrt{p^2+q^2}} \right]} \right]^2, \quad n = 0, 1, 2, \dots. \quad (34)$$

It seems that for $p = 0.7$ and $q = 0.3$, α_n is nearly the same as the exact α_n^E in Table 1. However, one finds that $\varphi_\infty \neq 0$ for $\alpha = \{\alpha_n\}$. This implies that $\{\alpha_n\}$ determined by the WKB method does not describe the asymptotically vanishing scalar clouds correctly. Hence, $\{\alpha_n\}$ do not represent bifurcation points precisely.

The infinite $n = 0, 1, 2, \dots$ black holes with $p = 0.7$ and $q = 0.3$ are defined by α -bounds of $\alpha \geq \alpha_0^E$, $\alpha \geq \alpha_1^E$, $\alpha \geq \alpha_2^E$, \dots , respectively. In addition, we confirm an inequality for $p = 0.7$ and $q = 0.3$ as

$$\alpha_{po} = 5.3404 < \alpha_0^E = \alpha_{th} = 8.86464 < \alpha_{in} = 9.4606. \quad (35)$$

3 Scalarized charged black holes

To obtain scalarized charged black holes through spontaneous scalarization, we introduce the metric and fields as [4]

$$ds_{\text{SCBH}}^2 = \bar{g}_{\mu\nu} dx^\mu dx^\nu = -N(r) e^{-2\delta(r)} dt^2 + \frac{dr^2}{N(r)} + r^2 (d\theta^2 + \sin^2 \theta d\varphi^2)$$

$$N(r) = 1 - \frac{2m(r)}{r}, \quad \bar{\phi} = \phi(r), \quad \bar{A}_t = v_Q(r), \quad \bar{B}_t = v_P(r). \quad (36)$$

Substituting (36) into (7)-(11), one has the five equations

$$\begin{aligned} & -2m'(r) + e^{2\delta(r)}r^2 \left(e^{-\alpha\phi(r)^2} (v'_Q(r))^2 + e^{\alpha\phi(r)^2} (v'_P(r))^2 \right) \\ & + r[r - 2m(r)](\phi'(r))^2 = 0, \end{aligned} \quad (37)$$

$$\delta'(r) + r(\phi'(r))^2 = 0, \quad (38)$$

$$v'_Q(r) \left(2 + r\delta'(r) - 2r\alpha\phi(r)\phi'(r) \right) + rv''_Q(r) = 0, \quad (39)$$

$$v'_P(r) \left(2 + r\delta'(r) + 2r\alpha\phi(r)\phi'(r) \right) + rv''_P(r) = 0, \quad (40)$$

$$\begin{aligned} & e^{2\delta(r)}r^2\alpha\phi(r) \left(e^{\alpha\phi(r)^2} (v'_P(r))^2 - e^{-\alpha\phi(r)^2} (v'_Q(r))^2 \right) + r[r - 2m(r)]\phi''(r) \\ & - \left(m(r)[2 - 2r\delta'(r)] + r[-2 + r\delta'(r) + 2m'(r)] \right) \phi'(r) = 0, \end{aligned} \quad (41)$$

where the prime (') denotes differentiation with respect to its argument.

Accepting the existence of a horizon located at $r = r_+$, one finds an approximate solution to equations (37)-(41) in the near-horizon

$$m(r) = \frac{r_+}{2} + m_1(r - r_+) + \dots, \quad \delta(r) = \delta_0 + \delta_1(r - r_+) + \dots, \quad (42)$$

$$v_Q(r) = v_{Q1}(r - r_+) + \dots, \quad v_P(r) = v_{P1}(r - r_+) + \dots, \quad (43)$$

$$\phi(r) = \phi_0 + \phi_1(r - r_+) + \dots, \quad (44)$$

where the five coefficients are given by

$$\begin{aligned} m_1 &= \frac{e^{-\alpha\phi_0^2}P^2 + e^{\alpha\phi_0^2}Q^2}{2r_+^2}, \quad \delta_1 = -r_+\phi_1^2, \\ \phi_1 &= \frac{\alpha\phi_0(P^2 - e^{2\alpha\phi_0^2}Q^2)}{r_+(P^2 + e^{2\alpha\phi_0^2}Q^2 - e^{\alpha\phi_0^2}r_+^2)}, \\ v_{Q1} &= -\frac{e^{-\delta_0 + \alpha\phi_0^2}Q}{r_+^2}, \quad v_{P1} = -\frac{e^{-\delta_0 - \alpha\phi_0^2}P}{r_+^2}. \end{aligned} \quad (45)$$

Here, two important parameters of $\phi_0 = \phi(r_+, \alpha)$ (See Fig.6) and $\delta_0 = \delta(r_+, \alpha)$ are determined when matching with an asymptotically flat solution in the far-region

$$\begin{aligned} m(r) &= M - \frac{P^2 + Q^2 + Q_s^2}{2r} + \dots, \quad \delta(r) = \frac{Q_s^2}{2r^2} + \dots, \\ v_P(r) &= \Phi_P + \frac{P}{r} + \dots, \quad v_Q(r) = \Phi_Q + \frac{Q}{r} + \dots, \\ \phi(r) &= \frac{Q_s}{r} + \dots, \end{aligned} \quad (46)$$

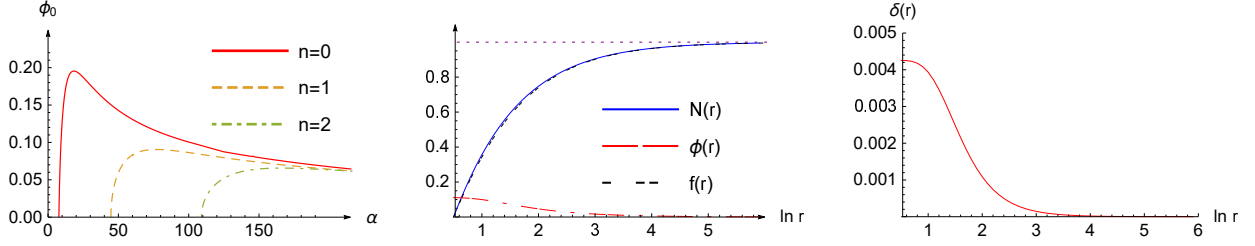


Figure 6: (Left) The scalar field $\phi_0 = \phi(r_+)$ at the horizon as function of α . The $n = 0$ fundamental branch starts from the first bifurcation point at $\alpha_0^E = 8.864$, while $n = 1, 2$ excited branches start from $\alpha_1^E = 44.663$ and $\alpha_2^E = 109.071$. (Middle and Right) Graphs of a scalarized charged black hole with $\alpha = 68.45$, $\phi_0 = 0.111$, and $\delta_0 = 0.0043$ in the $n = 0$ branch with $P = 0.7$ and $Q = 0.3$. Here $f(r)$ represents the metric function for the RN black hole with $\phi_{\text{RN}}(r) = 0$ and $\delta_{\text{RN}}(r) = 0$. We plot all figures in terms of $\ln r$ and thus, the horizon is always located at $\ln r = \ln r_+ = -0.153$.



Figure 7: $\bar{A}_t(r)$ and $\bar{B}_t(r)$ represent two vector potentials of RN black holes. $v_Q(r)$ and $v_P(r)$ represent vector potentials of scalarized charged black hole with $\alpha = 68.45$, $\Phi_P = -0.424$ and $\Phi_Q = -0.182$.

where Q_s , Φ_Q and Φ_P denote the scalar charge, and the electrostatic potentials at infinity, in addition to the ADM mass M , and the electric charges Q and P .

At this stage, we wish to comment that there is no constraint on P and Q in constructing scalarized charged black holes.

As an explicit scalarized charged black hole solution with $P = 0.7$ and $Q = 0.3$, we show a numerical black hole solution with $\alpha = 68.45$ in the $n = 0$ fundamental branch of $\alpha \geq 8.864$ in Figs. 6 and 7. However, we need hundreds of numerical solutions depending α for each branch to perform the stability of scalarized charged black holes.

4 Stability of scalarized charged black holes

The stability of scalarized charged black holes is an important question because it determines their viability in representing realistic astrophysical configurations. We prefer to introduce the radial perturbations around the scalarized black holes as

$$\begin{aligned} ds_{\text{rad}}^2 &= -N(r)e^{-2\delta(r)}(1 + \epsilon H_0)dt^2 + \frac{dr^2}{N(r)(1 + \epsilon H_1)} + r^2(d\theta^2 + \sin^2\theta d\psi^2), \\ H_{rt}(t, r) &= v'_P(r) + \epsilon\delta v_P(t, r), \quad F_{rt}(t, r) = v'_Q(r) + \epsilon\delta v_Q(t, r), \\ \phi(t, r) &= \phi(r) + \delta\tilde{\phi}(t, r), \end{aligned} \tag{47}$$

where $N(r)$, $\delta(r)$, $\phi(r)$, $v_P(r)$ and $v_Q(r)$ represent a scalarized charged black hole background, while $H_0(t, r)$, $H_1(t, r)$, $\delta\tilde{\phi}(t, r)$, $\delta v_P(t, r)$ and $\delta v_Q(t, r)$ denote five perturbed fields around the scalarized black hole background. From now on, we confine ourselves to analyzing the $l = 0$ (s-mode) propagation, implying that higher angular momentum modes ($l \neq 0$) are excluded. In this case, all perturbed fields except the perturbed scalar field may belong to redundant fields. After applying decoupling process to linearized equations, one may find a linearized scalar equation.

Considering the separation of variables

$$\delta\tilde{\phi}(t, r) = \frac{\tilde{\varphi}(r)e^{\Omega t}}{r}, \tag{48}$$

we obtain the Schrödinger-type equation for an s -mode scalar perturbation

$$\frac{d^2\tilde{\varphi}(r)}{dr_*^2} - \left[\Omega^2 + V(r, \alpha) \right] \tilde{\varphi}(r) = 0, \tag{49}$$

with r_* is the tortoise coordinate defined by

$$\frac{dr_*}{dr} = \frac{e^{\delta(r)}}{N(r)}. \tag{50}$$

Here, its potential reads to be

$$\begin{aligned} V(r, \alpha) &= \frac{N}{e^{2\delta}r^2} \left[(1 - N - 2r^2\phi'^2) + \frac{e^{-\alpha\phi^2}P^2[-\alpha - 1 + 2(-\alpha\phi + r\phi')^2]}{r^2} \right. \\ &\quad \left. + \frac{e^{\alpha\phi^2}Q^2[\alpha - 1 + 2(\alpha\phi + r\phi')^2]}{r^2} \right] \end{aligned} \tag{51}$$

whose limit of $Q^2 \rightarrow 0$ recovers the potential $U_\Omega(-\alpha)$ for the EMS theory in [4].

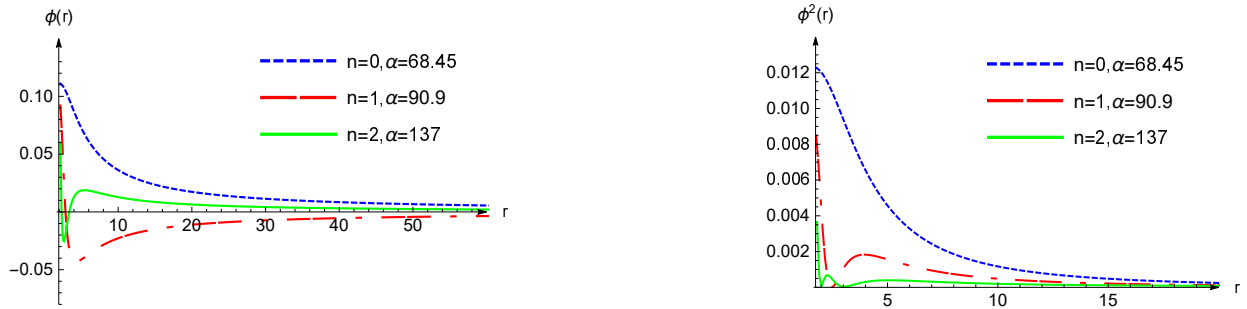


Figure 8: (Left) Scalar solution $\phi(r)$ and (Right) its square $\phi^2(r)$ as functions of $r \in [r_+ = 1.648, 50]$ for the first three branches with $P = 0.7$ and $Q = 0.3$. Here, we choose $\phi_0 = 0.111$, $Q_s = 0.3272$ for $n = 0$ branch ; $\phi_0 = 0.0921$, $Q_s = -0.2097$ for $n = 1$ branch; $\phi_0 = 0.0606$, $Q_s = 0.1222$, for $n = 2$ branch.

Before we proceed, we wish to analyze the potential $V(r, \alpha)$ carefully because it is a compact one. First of all, we observe that $V(r, \alpha)$ reduces to $V_{\text{RN}}(r)$ in (22) when imposing $\phi = \delta = 0[N(r) \rightarrow f(r)]$. This implies that ‘ $-\alpha P^2/r^2$ ’ in the second term contributes to a negatively large potential in the near-horizon as in the RN case (see Fig. 3), while the first and last terms make positively small contributions to the potential. Importantly, ‘ $2(-\alpha\phi + r\phi')^2 P^2/r^2$ ’ in the second term plays the role of making small positive region in the near-horizon as n increases. As is shown in Fig. 8 (similar to Fig. 4), the number of scalar-node increases as n increases, which implies that the positive (negative) region of ϕ^2 ($V(r, \alpha)$) decreases (increases) in the near-horizon. This may explain that the $n = 0$ ($\alpha \geq 8.864$) black hole is stable against the s -mode scalar perturbation, whereas the $n = 1$ ($\alpha \geq 44.67$), ($n = 2$ ($\alpha \geq 109.071$), 3 ($\alpha \geq 202.111$), 4 ($\alpha \geq 323.754$), \dots) excited black holes may be unstable.

The conclusions about the stability of the scalarized charged black holes with respect to radial perturbations will be reached by examining the qualitative behavior of the potential $V(r, \alpha)$ as well as by obtaining explicitly exponentially growing (unstable) modes for s -mode scalar perturbation. We display three scalar potentials $V(r, \alpha)$ in (Left) Fig. 9 for $l = 0$ (s -mode) scalar around the $n = 0$ black hole, showing positive definite. This implies that the $n = 0$ black hole is stable against the s -mode of perturbed scalar. We confirm its stability by noting negative Ω in Fig. 10. We observe from Fig. 9 that $\int_{r_+}^{\infty} dr [e^{\delta} V(r, \alpha)/N] < 0$ (sufficient condition for instability [17]) for the $n = 1, 2$ black holes. This suggests that the $n = 1, 2$ black holes are unstable against the s -mode scalar perturbation. Obviously,

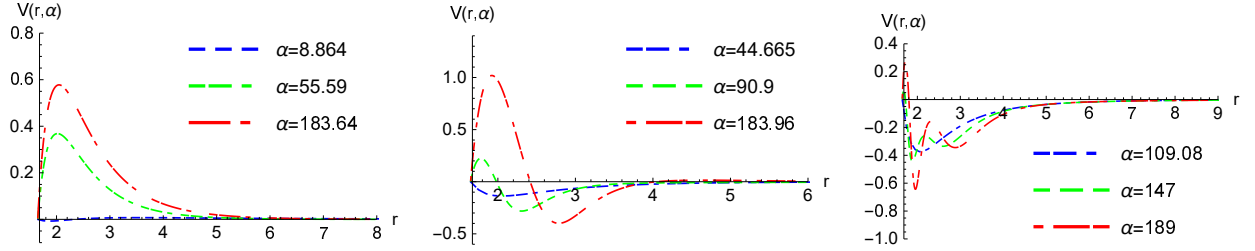


Figure 9: Scalar potentials $V(r, \alpha)$ around $n = 0$ (Left: $\alpha \geq 8.864$), 1 (Middle: $\alpha \geq 44.663$), 2 (Right: $\alpha \geq 109.071$) black holes in the infinite branches. The positive barriers in the near-horizon become smaller and smaller as n increases.

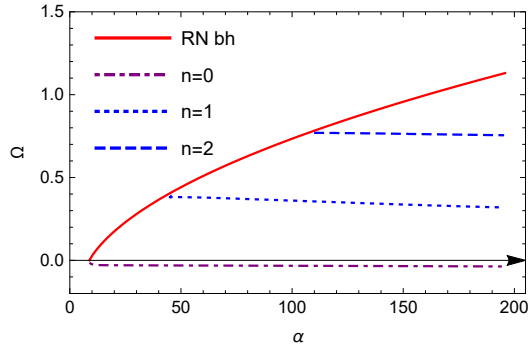


Figure 10: Plots of Ω as functions of α for $l = 0$ -scalar mode around the $n = 0$ ($\alpha \geq 8.864$), 1 ($\alpha \geq 44.663$), 2 ($\alpha \geq 109.071$) black holes with $P = 0.7$ and $Q = 0.3$. The positive Ω for $n = 1, 2$ black holes implies unstable black holes, while the negative Ω for the $n = 0$ black hole shows a stable black hole. A red curve started at $\alpha = 8.864$ ($\Omega = 0$) denotes the positive Ω , indicating the unstable RN black hole for $\alpha > 8.864$.

their instability are found from Fig. 10 in accordance with the existence of unstable modes because all (Ω) are positive. This is consistent with the results for the EMS theory with exponential coupling [19] and quadratic coupling [20], and for the EMCS theory with exponential and quadratic couplings [21]. The stability for a quartic coupling in the EMS theory was recently announced by considering full perturbations [22].

5 Discussions

First of all, let us compare a fixed scalar in the dilatonic black hole with scalar hairs in the scalarized charged black holes. Fig. 1 implies that the dilaton is a fixed scalar whose

value on the horizon is fixed by the U(1) charges Q and P and it is given independently by $\phi_\infty = 0$ at infinity. A scalar hair whose value on the horizon is fixed by two U(1) charges Q , P and α , and it is asymptotically zero. Hence, the fixed scalar is similar to the scalar hair.

Now, we would like to mention the stability of scalarized charged black holes. Firstly, we note that the RN black hole is unstable for $\alpha > \alpha_{\text{th}}$ (See Fig. 10), while it is stable for $\alpha < \alpha_{\text{th}}$. Here, α_{th} denotes the threshold of instability for RN black hole as well as it indicates the boundary between RN and $n = 0$ scalarized charged black holes. On the region ($\alpha \geq 8.864$) of unstable RN black holes, we could obtain the fundamental $n = 0$ ($\alpha \geq 8.864$) black hole, and $n = 1$ ($\alpha \geq 44.67$), ($n = 2$ ($\alpha \geq 109.071$), 3 ($\alpha \geq 202.111$), 4 ($\alpha \geq 323.754$), \dots excited black holes inspired by the onset of spontaneous scalarization.

The stability analysis of scalarized charged black holes is an important matter because it determines their viability in representing realistic astrophysical configurations. Also, it is not an easy task since one needs hundreds of numerical solutions depending α for each branch to perform the stability of scalarized charged black holes. It seems to be difficult for them to become stable ones because their defined areas correspond to region of unstable RN black holes without scalar hair (by making large negative region in the potential). Fortunately, one may have a stable black hole in the fundamental branch because there exists a positively scalar hair contribution of $'2(-\alpha\phi + r\phi')^2 P^2/r^2'$ to the potential (51). It turns out that the $n = 0$ black hole is stable against the $s(l = 0)$ -mode scalar perturbation, whereas the $n = 1, 2$ excited black holes are unstable. This is consistent with the results for the EMS theory with exponential coupling [19] and quadratic coupling [20].

On the other hand, the stability analysis of scalarized charged black holes can answer to whether they could be the endpoints of tachyonic instability of RN black holes without scalar hair. Since the $n = 0$ scalarized charged black hole is stable, this is regarded as an endpoint of the unstable RN black hole.

Acknowledgments

This work was supported by the National Research Foundation of Korea (NRF) grant funded by the Korea government (MOE) (No. NRF-2017R1A2B4002057).

References

- [1] D. D. Doneva and S. S. Yazadjiev, *Phys. Rev. Lett.* **120**, no. 13, 131103 (2018) doi:10.1103/PhysRevLett.120.131103 [arXiv:1711.01187 [gr-qc]].
- [2] H. O. Silva, J. Sakstein, L. Gualtieri, T. P. Sotiriou and E. Berti, *Phys. Rev. Lett.* **120**, no. 13, 131104 (2018) doi:10.1103/PhysRevLett.120.131104 [arXiv:1711.02080 [gr-qc]].
- [3] G. Antoniou, A. Bakopoulos and P. Kanti, *Phys. Rev. Lett.* **120**, no. 13, 131102 (2018) doi:10.1103/PhysRevLett.120.131102 [arXiv:1711.03390 [hep-th]].
- [4] C. A. R. Herdeiro, E. Radu, N. Sanchis-Gual and J. A. Font, *Phys. Rev. Lett.* **121**, no. 10, 101102 (2018) doi:10.1103/PhysRevLett.121.101102 [arXiv:1806.05190 [gr-qc]].
- [5] P. G. S. Fernandes, C. A. R. Herdeiro, A. M. Pombo, E. Radu and N. Sanchis-Gual, *Class. Quant. Grav.* **36**, no. 13, 134002 (2019) Erratum: [*Class. Quant. Grav.* **37**, no. 4, 049501 (2020)] doi:10.1088/1361-6382/ab685c, 10.1088/1361-6382/ab23a1 [arXiv:1902.05079 [gr-qc]].
- [6] D. Astefanesei, C. Herdeiro, A. Pombo and E. Radu, *JHEP* **1910**, 078 (2019) doi:10.1007/JHEP10(2019)078 [arXiv:1905.08304 [hep-th]].
- [7] B. Kol and A. Rajaraman, *Phys. Rev. D* **56**, 983 (1997) doi:10.1103/PhysRevD.56.983 [hep-th/9608126].
- [8] M. Krasnitz and I. R. Klebanov, *Phys. Rev. D* **56**, 2173 (1997) doi:10.1103/PhysRevD.56.2173 [hep-th/9703216].
- [9] H. W. Lee, Y. S. Myung and J. Y. Kim, *Phys. Lett. B* **410**, 6 (1997) doi:10.1016/S0370-2693(97)00794-6 [hep-th/9704199].
- [10] S. Ferrara, R. Kallosh and A. Strominger, *Phys. Rev. D* **52**, R5412 (1995) doi:10.1103/PhysRevD.52.R5412 [hep-th/9508072].
- [11] S. Ferrara and R. Kallosh, *Phys. Rev. D* **54**, 1525 (1996) doi:10.1103/PhysRevD.54.1525 [hep-th/9603090].
- [12] Y. S. Myung and D. C. Zou, *Eur. Phys. J. C* **79**, no. 3, 273 (2019) doi:10.1140/epjc/s10052-019-6792-6 [arXiv:1808.02609 [gr-qc]].

- [13] F. J. Zerilli, Phys. Rev. D **9**, 860 (1974). doi:10.1103/PhysRevD.9.860
- [14] V. Moncrief, Phys. Rev. D **9**, 2707 (1974). doi:10.1103/PhysRevD.9.2707
- [15] V. Moncrief, Phys. Rev. D **10**, 1057 (1974). doi:10.1103/PhysRevD.10.1057
- [16] V. Moncrief, Phys. Rev. D **12**, 1526 (1975). doi:10.1103/PhysRevD.12.1526
- [17] G. Dotti and R. J. Gleiser, Class. Quant. Grav. **22**, L1 (2005) doi:10.1088/0264-9381/22/1/L01 [gr-qc/0409005].
- [18] S. Hod, Phys. Lett. B **798**, 135025 (2019) [arXiv:2002.01948 [gr-qc]].
- [19] Y. S. Myung and D. C. Zou, Phys. Lett. B **790**, 400 (2019) doi:10.1016/j.physletb.2019.01.046 [arXiv:1812.03604 [gr-qc]].
- [20] Y. S. Myung and D. C. Zou, Eur. Phys. J. C **79**, no. 8, 641 (2019) doi:10.1140/epjc/s10052-019-7176-7 [arXiv:1904.09864 [gr-qc]].
- [21] D. C. Zou and Y. S. Myung, arXiv:2005.06677 [gr-qc].
- [22] J. L. Blzquez-Salcedo, C. A. R. Herdeiro, S. Kahlen, J. Kunz, A. M. Pombo and E. Radu, arXiv:2008.11744 [gr-qc].